Supplemental File

The DEL-1–β3 integrin axis promotes regulatory T cell responses during inflammation resolution

Xiaofei Li[1,§], Alessandra Colamatteo[2,§], Lydia Kalafati[3,4], Tetsuhiro Kajikawa[1], Hui Wang[1], Jong-Hyung Lim[1], Khalil Bdeir[5], Kyoung-Jin Chung[3], Xiang Yu[6], Clorinda Fusco[2], Antonio Porcellini[7], Salvatore De Simone[8], Giuseppe Matarese[2,8], Triantafyllos Chavakis[3,‡], Veronica De Rosa[8,9,‡,*], and George Hajishengallis[1,‡,*]

[1] Department of Basic and Translational Sciences, Laboratory of Innate Immunity and Inflammation, Penn Dental Medicine, University of Pennsylvania, Philadelphia, PA, USA.
[2] Treg Cell Lab, Dipartimento di Medicina Molecolare e Biotecnologie Mediche, Università degli Studi di Napoli "Federico II", Napoli, Italy.
[3] Institute for Clinical Chemistry and Laboratory Medicine, Faculty of Medicine, Technische Universität Dresden, Dresden, Germany.
[4] National Center for Tumor Diseases, Dresden, and German Cancer Research Center, Heidelberg, Germany.
[5] Department of Pathology and Laboratory Medicine, Perelman School of Medicine, University of Pennsylvania, Philadelphia, PA, USA.
[6] Department of Biology, University of Pennsylvania, Philadelphia, PA, USA.
[7] Dipartimento di Biologia, Università degli Studi di Napoli "Federico II", Complesso Universitario di Monte Santangelo, Napoli, Italy.
[8] Istituto per l'Endocrinologia e l'Oncologia Sperimentale, Consiglio Nazionale delle Ricerche (IEOS-CNR), Napoli, Italy.
[9] Unità di Neuroimmunologia, Fondazione Santa Lucia, Roma, Italy.
§ These authors contributed equally to the work
‡ These authors contributed equally as senior authors to the work
* Corresponding authors. E-mail: veronica.derosa@cnr.it (VDR); geoh@upenn.edu (GH)

This file includes:

Supplemental Materials and Methods

Ligature-induced periodontitis / resolution model and cell isolation

Ligature-induced periodontitis and resolution thereof was performed in mice as previously described (1, 2). Briefly, a 5-0 silk ligature was tied around the maxillary left second molar and the ligatures were removed on day 10 for 5 days. The mice were euthanized on day 10 or day 15. The contralateral molar tooth in each mouse was left unligated (baseline control). Starting on the day of ligature removal, DEL-1-Fc, mutants thereof, or Fc control were intra-gingivally microinjected daily at the ligated sites for a total of five doses. Gingival tissues around the area of ligature placement (and the contralateral control area) and cLNs were harvested on day 15 for analysis. On day 15, gingiva was dissected around the area of ligature placement and digested for 1h at 37°C with RPMI 1640 medium (Gibco) supplemented with collagenase IV (3.2 mg/ml, Gibco) and DNase (0.15 μg/ml, Sigma-Aldrich) (3). Single-cell suspensions were obtained by mashing the tissue against a strainer using plungers and filtered for staining and flow cytometry.

Acute lung injury model

Acute lung injury was induced as previously described (4). Briefly, after anesthesia with intraperitoneal ketamine and acetylpromazine, mice were instilled intratracheally with *Escherichia coli* LPS (3.75 μg/g mouse; O55:B5, Sigma-Aldrich) or PBS control via a 20-gauge catheter. Mice were sacrificed on day 10. BAL was obtained by cannulating the trachea with a 20-gauge catheter. The lung was lavaged with calcium-free PBS three times (each aliquot 0.7 ml). BAL was centrifuged at 600x*g* for 10 mins at 4°C. Total protein concentration in cell-free supernatants was measured by the Bradford method. Total cell number was counted with a hemocytometer after staining with trypan blue. Treg and Th17 cell numbers and frequencies in BAL and draining LNs were determined by FACS. For lung histology, after formalin fixation, lungs were embedded in

paraffin and 5-μm sections were stained with hematoxylin and eosin. Lung injury was histologically evaluated by two investigators in a blinded fashion according to a semiquantitative scoring system (4): 1, normal; 2, focal (<50% of lung section) interstitial congestion and inflammatory cell infiltration; 3, diffuse (>50% of lung section) interstitial congestion and inflammatory cell infiltration; 4, focal (<50% of lung section) consolidation and inflammatory cell infiltration; 5, diffuse (>50% of lung section) consolidation and inflammatory cell infiltration (4). Data shown are the results from three representative sections of each mouse and the mean score was used for comparison between groups.

Proteins

Full-length human DEL-1 as a fusion protein with the human IgG1-Fc fragment (DEL-1−Fc), DEL-1 lacking the discoidin I-like domains (DEL-1[E1-E3]-Fc), and a point mutant of DEL-1 in which Asp [D] was replaced by Glu [E] in the RGD motif of the second EGF repeat (DEL-1[RGE]-Fc) were generated and purified as previously described (5). Fc protein control was purchased from R&D Systems. As human and mouse DEL-1 share 96% a.a. sequence and the two proteins have similar functions (2, 5-7), human DEL-1 was used in both human and mouse experimental systems.

Mouse flow cytometry and antibodies

Antibodies to the following mouse molecules were purchased from BioLegend: CD45 (clone 30-F11, catalog 103131), CD3 (145-2C11, catalog 100307), CD4 (GK1.5, catalog 100413, 100407), IL-17A (TC11-18H10.1, catalog 506916), CD51 (RMV-7, catalog 104105), CD61 (2C9.G2 [HMβ3-1], catalog 104315), CD44 (IM7, catalog 103005), CD62L (MEL-14, catalog 104407), CD25 (3C7, catalog 101912), CD8 (53-6.7, catalog 100721), IL-10 (JES5-16E3, catalog 505007), ICOS (7E.17G9, catalog 117405), CTLA-4 (UC10-4B9, catalog 106309) and RUNX1 (RXDMC, catalog 12-9816-80) from eBioscience. Function-blocking antibody to αvβ3 integrin (23C6, catalog 16-

104 0519-81) and IgG1 kappa isotype control (P3.6.2.8.1, catalog 16-4714-82) were from Invitrogen.
105 Anti-mouse FOXP3 (clone FJK-16s, catalog 11-5773-82) was from eBioscience and Live/Dead
106 fixable violet dead cell stain kit from Invitrogen. Mouse $CD4^+$ cells were stimulated or not with
107 PMA (50 ng/ml; Sigma-Aldrich) and ionomycin (1.0 µg/ml; Sigma-Aldrich) in the presence of BD
108 GolgiPlug (1 µl/ml media) for 3.5 hr at 37°C and 5% CO2. Then, following incubation with live/dead
109 fixable dye (Invitrogen) to exclude dead cells, live cells were treated with low-endotoxin and azide-
110 free purified anti-mouse CD16/32 antibody to block Fcγ III/II receptors (1:100; clone 93, catalog
111 101330, BioLegend) for 10 mins at 4°C in the dark. Cells were then stained for surface markers
112 for 30 mins at 4°C in the dark. The stained cells were further washed and fixed overnight. For
113 intracellular staining of IL-17A, cells were permeabilized with intracellular fixation and
114 permeabilization buffer set (eBioscience). For intracellular staining of FOXP3 alone or together
115 with IL-10 or RUNX1, the cells were fixed and permeabilized with Foxp3/transcription factor
116 staining buffer set (eBioscience). Cell acquisition was performed on a NovoCyte flow cytometer
117 (ACEA Biosciences). Data were analyzed with NovoExpress® software (ACEA Biosciences) and
118 FlowJo software (version 7.6.5, Tree Star).
119
120 **Quantitative real-time PCR**
121 Total cellular RNA was isolated from mouse tissues using Trizol (Life Technologies). For real-
122 time PCR, 500 ng of total RNA was reverse-transcribed using High-Capacity RNA-to-cDNA Kit
123 (Applied Biosystems) and real-time PCR with cDNA was performed using the Applied Biosystems
124 7500 Fast Real-Time PCR System according to the manufacturer's protocol (Applied
125 Biosystems). TaqMan probes and gene-specific primers (Supplemental Table 1; Thermo-Fisher)
126 for detection and quantification of murine genes investigated in this study were purchased from
127 Thermo-Fisher. Data were analyzed using the comparative (ΔΔCt) method. For studies in the
128 human system, total RNA was extracted from DEL-1-Fc- or Fc control-treated human iTregs using
129 RNAqueous-4PCR (Thermo-Fisher). cDNA was synthetized in a 20 µl reaction volume containing

1 µg of total RNA, SuperScript IV VILO (Thermo-Fisher) or 200 units of SuperScript III Reverse Transcriptase (Thermo-Fisher) and 0.5 µl of random primers (200 ng/µl) (Roche). *FOXP3* all transcripts, *FOXP3* splicing variants containing the exon 2 (*FOXP3E2*), *RUNX1* and *CBFB* mRNAs were detected by using Taqman Universal Master Mix II, with UNG (Thermo-Fisher) according to the manufacturer's instruction, and analyzed with StepOnePlus™ Real-Time PCR System (Thermo-Fisher) or QuantStudio3 Real-Time PCR System (Thermo-Fisher). The internal probes assays have been designed over exon 1 - exon 2 boundaries to detect FOXP3E2, over exon 9 - exon 10 boundaries (a region not undergoing splicing) to detect FOXP3 all transcripts. As internal standard control to perform normalization between samples, we used *18S* ribosomal RNA. TaqMan probes and gene-specific primers were from Thermo-Fisher (Supplemental Table 1). The mRNA expression was expressed as relative amount compared to *18S* RNA using the ΔCt method ($2^{-\Delta Ct}$); ΔCt is the difference in Ct between the gene of interest (*FOXP3* all transcripts, *FOXP3E2*, *RUNX1* and *CBFB*) and the endogenous control (*18S* RNA).

Human T cell flow cytometry, proliferation and CFSE staining

Flow cytometric analysis of T cells was performed essentially as previously described (8). Tconv cells, stimulated for 36 hrs with anti-CD3/anti-CD28 mAb-coated beads (0.1 bead per cell; Thermo-Fisher) in the presence of DEL-1-Fc or Fc control (both at 10 µg/ml), were surface-stained with the following mAbs: APC-H7-conjugated anti-human CD4 (RPA-T4, catalog 560158), PE-Cy7-conjugated anti-human CD25 (M-A251, catalog 557741), both from BD Biosciences. Thereafter, cells were washed, fixed and permeabilized (Human Foxp3 Buffer Set; BD Pharmingen) and stained with following mAbs: PE-conjugated anti-human FOXP3 from BD Biosciences (259D/C7, catalog 560046) that recognizes all splicing variants of FOXP3 (through an epitope of the amino terminus of FOXP3), and PE-conjugated anti-human FOXP3 from Thermo-Fisher (150D/E4, catalog 12-4774-42) that recognizes FOXP3E2 through an epitope

present in the exon 2 only. Cells were analyzed with FACSCanto II (BD Biosciences). Analysis was performed with FlowJo software (versions 10.0.7 and 10.1, Tree Star). For T cell proliferation and suppression assays, $CD4^+$ T cells (90-95% pure) (2×10^4 cells per well) from healthy subjects were purified by magnetic cell separation with Dynabeads Untouched Human CD4 T Cells Kit (Thermo-Fisher). The fluorescent dye CFSE was used at a concentration of 1 µg/ml (Invitrogen). Flow cytometry analyzing CFSE dilution was performed by gating on $CD4^+CFSE^+$ cells stimulated for 72 hrs in round-bottomed 96-well plates (Corning Falcon) with anti-CD3/anti-CD28 mAb-coated beads (0.2 bead per cell; Thermo-Fisher) alone or cultured with DEL-1-Fc–iTregs or Fc–iTregs.

Methylation experiments

The methylation status of the CpG island (specifically of the CpG motifs 394 and 224 as indicated by Floess et al (9) and corresponding to recognition sites for MspI and HpaII) within the CNS2 region of *FOXP3* was evaluated in (i) human FACS-sorted iTregs cultured for 10 days with anti-CD3/anti-CD28 and IL-2 and (ii) sorted mouse iTregs cultured for 4 days with anti-CD3/anti-CD28 and IL-2 plus TGFβ1, in the presence of DEL-1-Fc or Fc control. Genomic DNA was extracted by using PureLink™ Genomic DNA Mini Kit (Thermo-Fisher). The methylation of the FOXP3-CNS2 locus was determined using a method modified by von Kanel et al (10). Briefly, genomic DNA (1 µg) isolated from cells was digested overnight at 37°C with 20 U SacI and 20 U of HpaII or 10 U of MspI (BioLabs). On the same digestion, *FOXP3*, *H19* and *UBE2B* CpG islands were analyzed by QuantStudio3 Real-Time PCR System (Thermo-Fisher) with specific primer (Supplemental Table 2). *H19* (imprinted locus) and *UBE2B* (unmethylated locus) were used as control. Data were analyzed using the comparative (ΔCt) method. The degree of methylation of each locus was assigned according to the following equation: Methylation percentage = $2^{\wedge(Ctsham-CtHpaII)}x100$, where CtHpaII and Ctsham are the Cts of the reactions performed with and without HpaII, respectively.

The assay performance was assessed on internal controls from the same digestion (same tube): for each sample a scatterplot was constructed using the *H19* ΔCt (Ctsham-CtHpaII). A logarithmic trend line was constructed and the equation obtained was used to interpolate the ΔCt of CNS2. Results were calculated as % methylation of the CNS2 region.

References for Supplemental Material and Methods

1. Abe T, Hajishengallis G. Optimization of the ligature-induced periodontitis model in mice. *J Immunol Methods*. 2013;394(1-2):49-54.
2. Kourtzelis I, et al. DEL-1 promotes macrophage efferocytosis and clearance of inflammation. *Nat Immunol*. 2019;20(1):40-49.
3. Dutzan N, Abusleme L, Konkel JE, Moutsopoulos NM. Isolation, Characterization and Functional Examination of the Gingival Immune Cell Network. *J Vis Exp*. 2016;(108):53736.
4. D'Alessio FR, et al. CD4+CD25+Foxp3+ Tregs resolve experimental lung injury in mice and are present in humans with acute lung injury. *J Clin Invest*. 2009;119(10):2898-2913.
5. Shin J, et al. DEL-1 restrains osteoclastogenesis and inhibits inflammatory bone loss in nonhuman primates. *Sci Transl Med*. 2015;7(307):307ra155.
6. Choi EY, et al. Del-1, an endogenous leukocyte-endothelial adhesion inhibitor, limits inflammatory cell recruitment. *Science*. 2008;322(5904):1101-1104.
7. Eskan MA, et al. The leukocyte integrin antagonist Del-1 inhibits IL-17-mediated inflammatory bone loss. *Nat Immunol*. 2012;13(5):465-473.
8. De Rosa V, et al. Glycolysis controls the induction of human regulatory T cells by modulating the expression of FOXP3 exon 2 splicing variants. *Nat Immunol*. 2015;16(11):1174-1184.
9. Floess S, et al. Epigenetic control of the foxp3 locus in regulatory T cells. *PLoS Biol*. 2007;5(2):e38.
10. von Kanel T, et al. Quantitative 1-Step DNA Methylation Analysis with Native Genomic DNA as Template. *Clin Chem*. 2010;56(7):1098-1106.

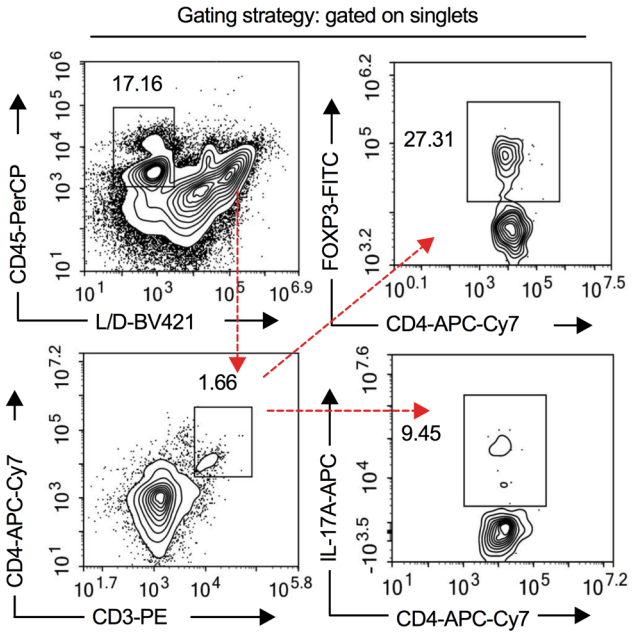

Supplemental Figure 1. Flow cytometry gating strategy for oral tissues. Groups of wild-type (WT) mice were subjected to ligature-induced periodontitis for 10 days and ligatures were removed on day 10 for 5 days to enable inflammation resolution. Representative FACS plot showing the gating strategy for Treg and Th17 cells present in WT mouse gingival tissues on day 15. FACS analysis of cervical lymph nodes followed the same strategy.

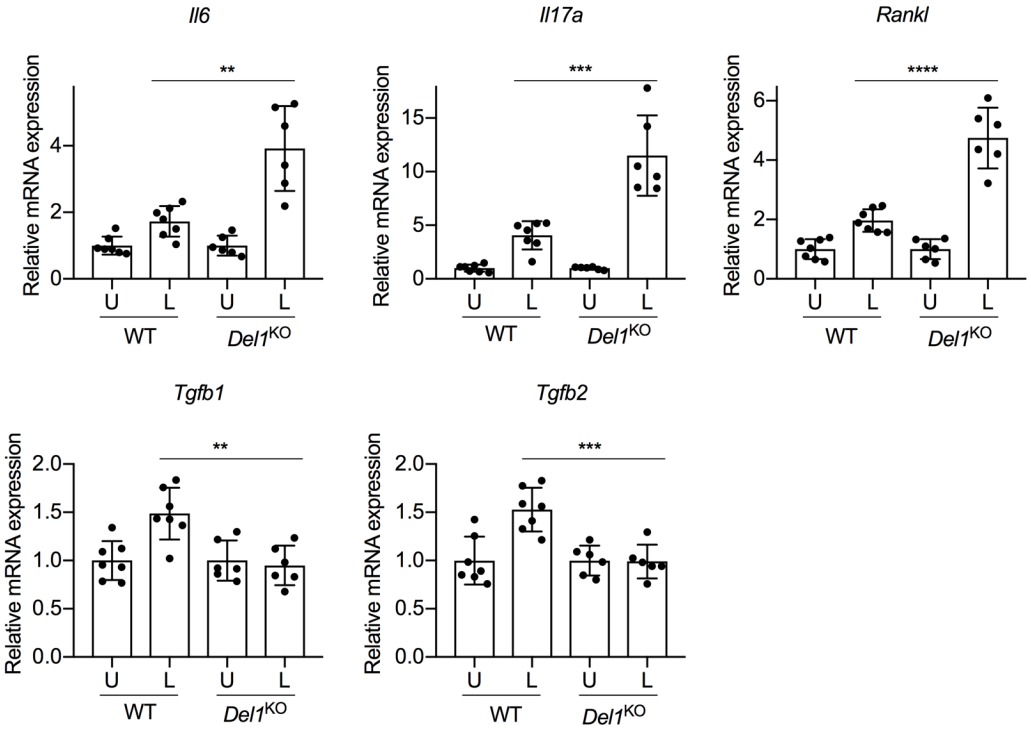

Supplemental Figure 2. Impaired resolution of periodontal inflammation in DEL-1–deficient mice. Groups of littermate wild-type (WT) and *Del1*^{KO} mice were subjected to ligature-induced periodontitis (LIP) for 10 days and ligatures were removed on day 10 for 5 days. Relative mRNA expression of indicated molecules in gingival tissues of littermate WT and *Del1*^{KO} mice on day 15 (*n*=7 mice for WT group and *n*=6 mice for KO group). Data were normalized to *Gapdh* mRNA and are presented as fold change relative to baseline (unligated sites), set as 1. Data are means ± SD and are pooled from two independent experiments. ***P*<0.01, ****P*<0.001, *****P*<0.0001 vs. ligated sides of WT mice. Two-tailed Student's t-test. U, unligated; L, ligated.

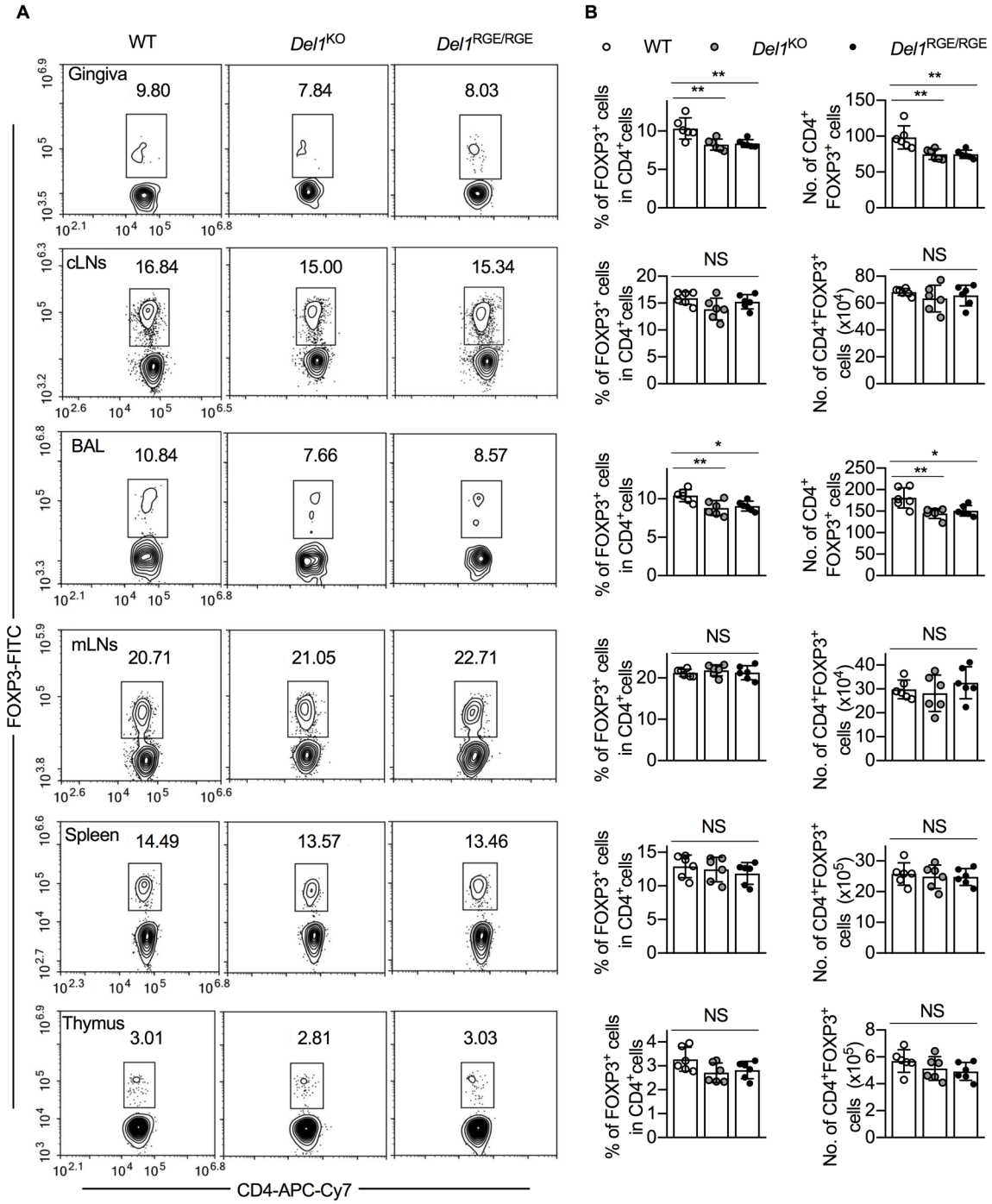

Supplemental Figure 3. Treg frequencies and absolute numbers in gingiva, BAL, LNs, spleen and thymus under the steady state condition. Treg frequencies and absolute numbers in groups of wild-type (WT), *Del1*^{KO} or *Del1*$^{RGE/RGE}$ mice were determined by FACS analysis. **(A)** Representative FACS plot of Treg cells; **(B)** data analysis of the percentages and absolute numbers of Treg cells.

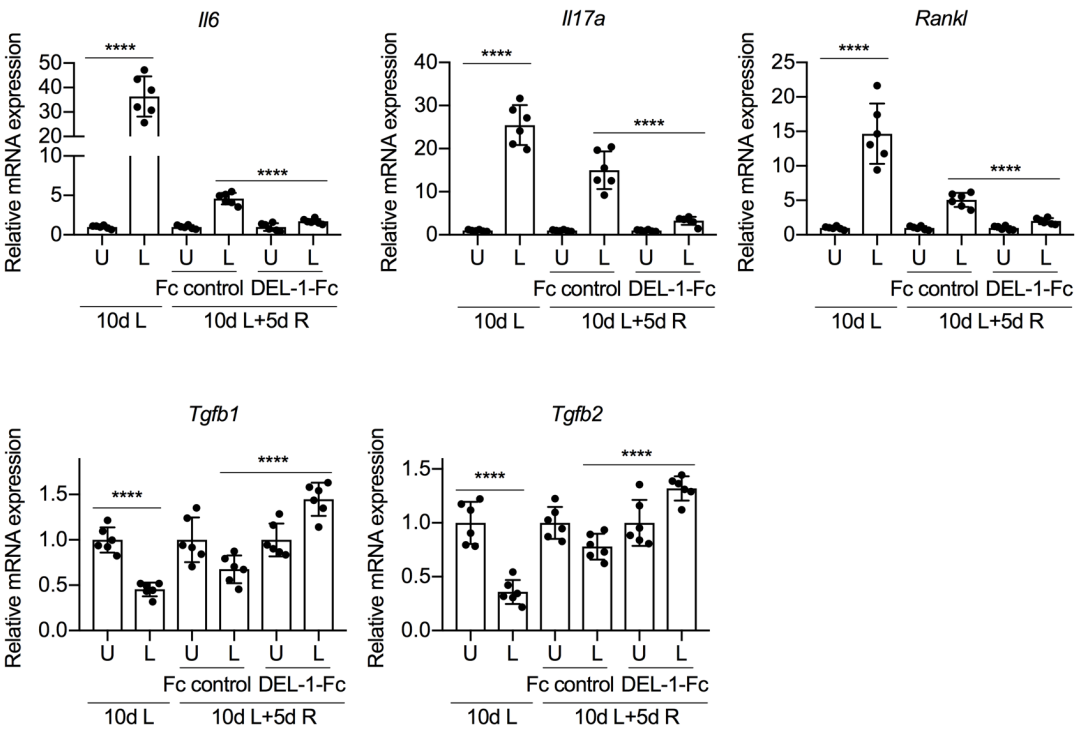

Supplemental Figure 4. DEL-1-Fc promotes inflammation resolution in periodontitis. Groups of *Del1*^{KO} mice were subjected to ligature-induced periodontitis (LIP) for 10 days. One group was euthanized at day 10 for dissecting gingiva for cytokine expression analysis (10d L group). In two other groups subjected to LIP, the ligatures were removed on day 10 for another 5 days to enable resolution (10dL +5dR groups). After ligature removal, the 10dL +5dR groups of mice were locally microinjected daily with DEL-1-Fc or Fc control from day 10 to day 14 for a total of 5 doses. Relative mRNA expression of the indicated molecules in the gingival tissue of the various groups was determined by quantitative real-time PCR. Data were normalized to *Gapdh* mRNA and are presented as fold change relative to baseline (unligated sites), set as 1. Data are means ± SD (*n*=6 mice per group and are pooled from two independent experiments each with three mice/group). ****P<0.0001 between indicated groups. Two-tailed Student's *t*-test. U, unligated; L, ligated.

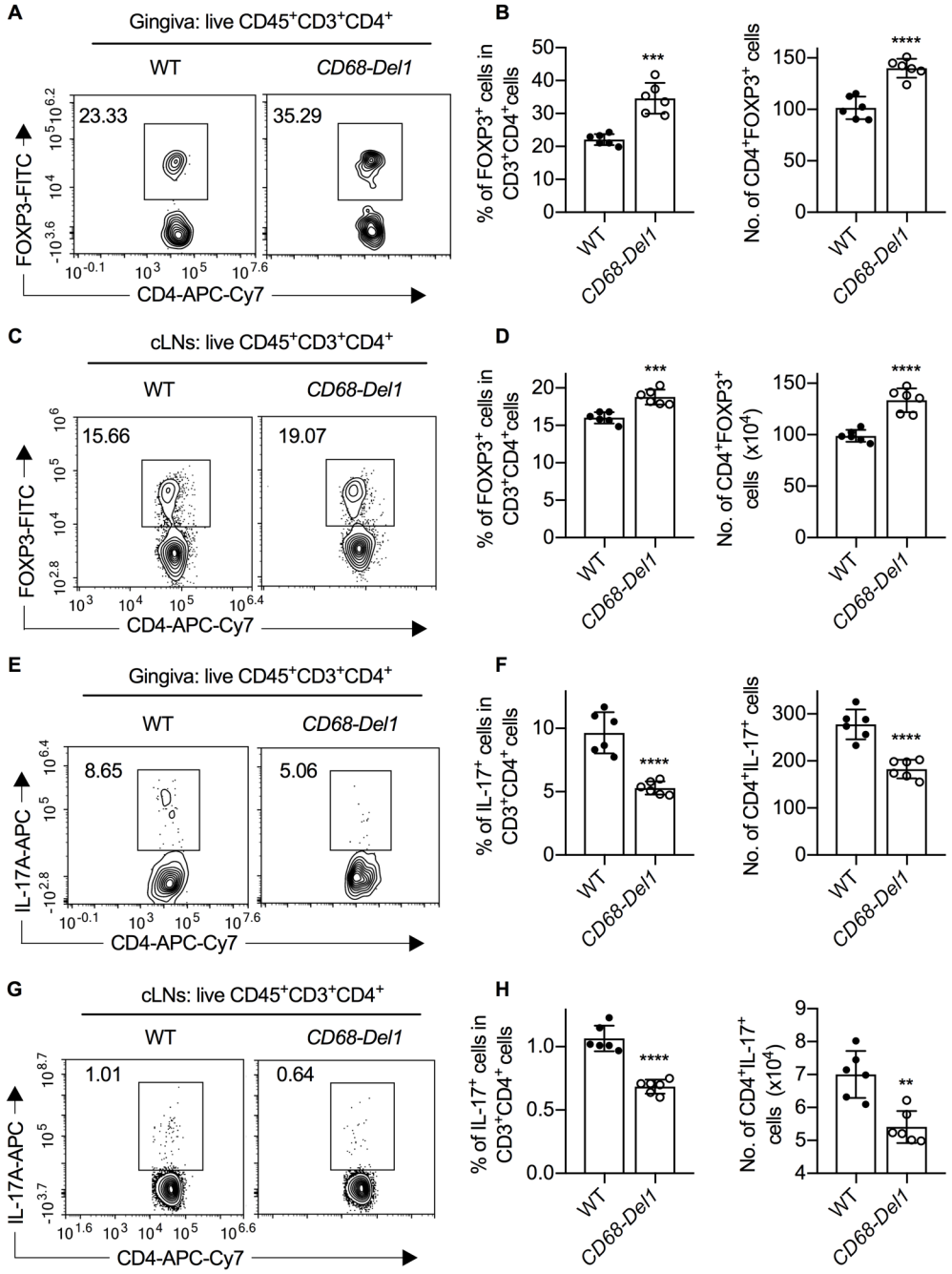

Supplemental Figure 5. Macrophage-derived DEL-1 increases Treg cells numbers while decreasing Th17 cells during resolution of inflammation. Groups of littermate wild-type (WT) and *CD68-Del1* mice were subjected to ligature-induced periodontitis (LIP) for 10 days and ligatures were removed on day 10 (to facilitate inflammation resolution) for 5 days. **(A)** Representative FACS plots of Treg cells in gingival tissue on day 15 and (**B**) bar graphs showing percentage of Treg cells in $CD4^+$ T cells (left) and absolute numbers of Treg cells (right) from gingival tissues of indicated mouse groups on day 15 (*n*=6 mice per group). (**C**) Representative FACS plot of Treg cells in cervical lymph nodes (cLNs) on day 15 and **(D)** bar graphs showing percentage of Treg cells in $CD4^+$ T cells (left) and absolute numbers of Treg cells (right) from

cLNs of indicated mouse groups on day 15 (*n*=6 mice per group). **(E)** Representative FACS plots of Th17 cells in gingival tissue on day 15 and (**F**) bar graphs showing percentage of Th17 cells in $CD4^+$ T cells (left) and absolute numbers of Th17 cells (right) from gingival tissues of indicated mouse groups on day 15 (*n*=6 mice per group). (**G**) Representative FACS plot of Th17 cells in cLNs and **(H)** bar graphs showing percentage of Th17 cells in $CD4^+$ T cells (left) and absolute numbers of Th17 cells (right) from cLNs of of indicated mouse groups on day 15 (*n*=6 mice per group). Data are means ±SD and are pooled from two independent experiments. ***P*<0.01, ****P*<0.001, *****P*<0.0001 vs. WT mice; two-tailed Student's *t*-test.

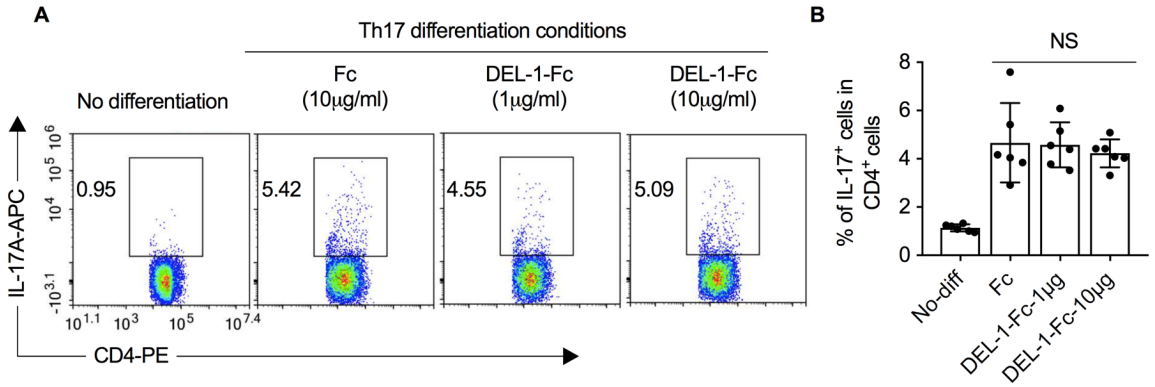

Supplemental Figure 6. DEL-1 has no direct effect on in vitro Th17 differentiation (IL-6+TGFβ1 condition). Naive splenic $CD4^+$ cells isolated from WT mice were differentiated, or not, to Th17 in medium containing anti-CD3/anti-CD28, TGFβ1 (1 ng/ml) and IL-6 (50 ng/ml) in the presence of the indicated concentrations of DEL-1-Fc or Fc control. Shown are **(A)** representative FACS plots and **(B)** data analysis of the percentage of $IL\text{-}17A^+$ cells in $CD4^+$ T cells from the in vitro culture system (*n*=6 replicates from two separate cell isolations). Data are means ± SD and are pooled from two independent experiments. NS, non-significant vs. Fc control group. One-way ANOVA with Dunnett's multiple comparisons test.

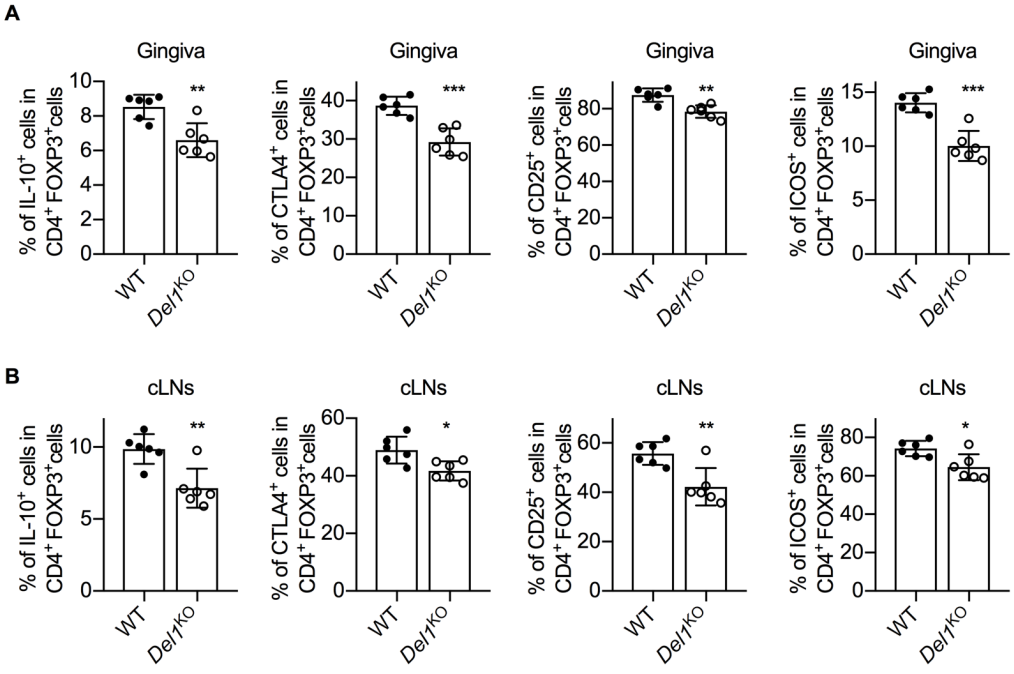

Supplemental Figure 7. **Endogenous DEL-1 promotes IL-10, CTLA-4, CD25 and ICOS expression in Treg cells in vivo.** Groups of littermate wild-type (WT) and *Del1*^{KO} mice were subjected to ligature-induced periodontitis (LIP) for 10 days and ligatures were removed on day 10 (to facilitate inflammation resolution) for 5 days. **(A)** Percentages of IL-10, CTLA-4, CD25 and ICOS expression in Treg cells from mice gingiva (*n*=6 mice per group). **(B)** Percentages of IL-10, CTLA-4, CD25 and ICOS expression in Treg cells from mice cLNs (*n*=6 mice per group). Data are means ±SD and are pooled from two independent experiments. **P*<0.05, ***P*<0.01, ****P*<0.001 vs. WT mice; two-tailed Student's *t*-test.

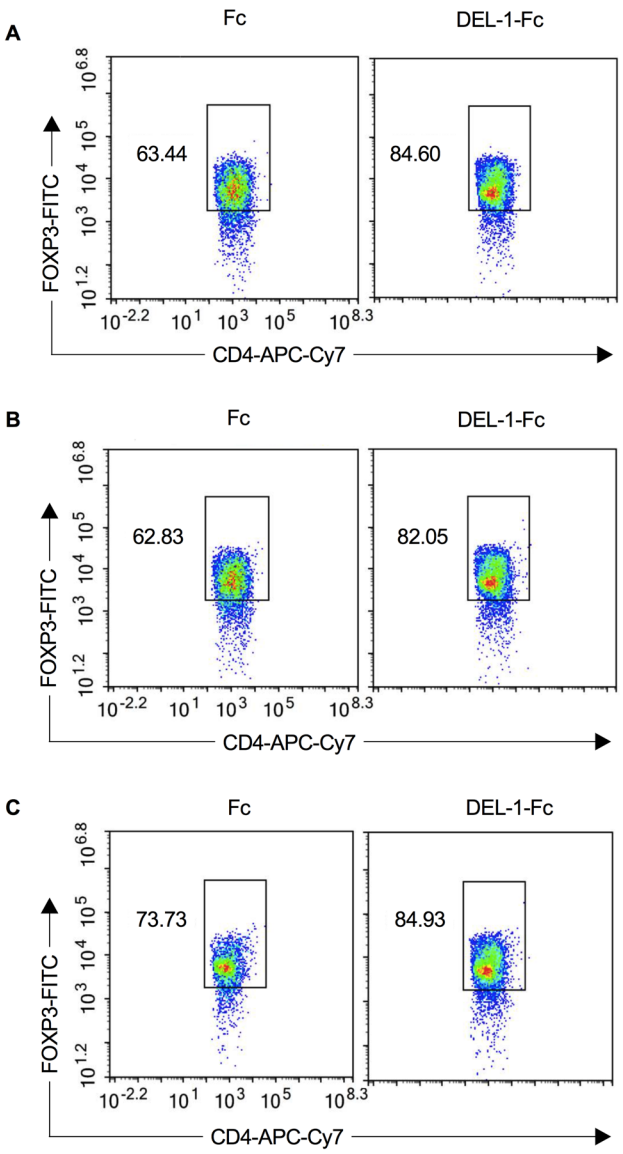

Supplemental Figure 8. **DEL-1 enhances FOXP3 stability. (A)** Naive splenic $CD4^+$ cells isolated from WT mice were differentiated to Treg cells in medium containing anti-CD3/anti-CD28, TGFβ1 (5 ng/ml) and IL-2 (40 ng/ml) in the presence of DEL-1-Fc or Fc control (all at 10 μg/ml). $CD4^+CD25^+$ cells were sorted and restimulated in medium containing IL-2 (40 ng/ml) for 4 days. Shown are representative FACS plots of FOXP3 expression. **(B,C)** Naive splenic $CD4^+$ cells isolated from WT mice were differentiated to Treg cells in medium containing anti-CD3/anti-CD28, TGFβ1 (5 ng/ml) and IL-2 (40 ng/ml), $CD4^+CD25^+$ cells were sorted and restimulated with DEL-1-Fc or Fc control in medium containing IL-2 (40 ng/ml) alone **(B)** or with TGFβ1 (5 ng/ml) **(C)** for 4 days. Shown are representative FACS plots of FOXP3 expression.

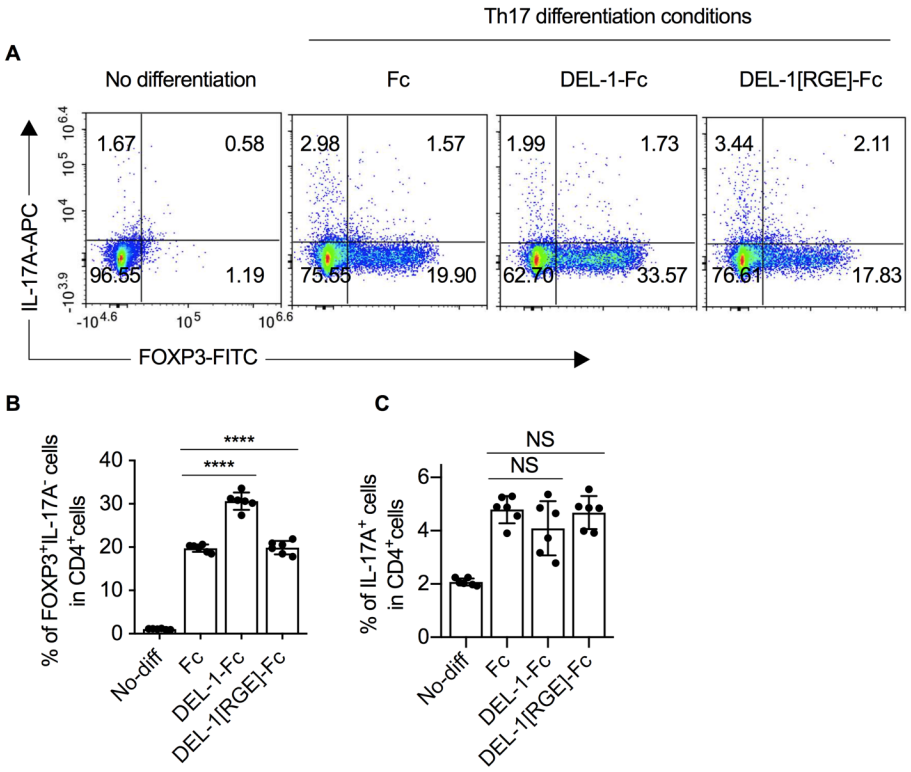

Supplemental Figure 9. DEL-1 promotes FOXP3 expression in T cells cultured under Th17 differentiation conditions. Naive splenic $CD4^+$ cells isolated from WT mice were cultured under Th17 differentiation conditions (medium containing anti-CD3/anti-CD28, 1 ng/ml TGFβ1 and 50 ng/ml IL-6) in the presence of 10 μg/ml of DEL-1-Fc, DEL-1[RGE]-Fc or Fc control. Shown are **(A)** representative FACS plots and data analysis of the percentage of **(B)** $FOXP3^+IL\text{-}17A^-$ cells and **(C)** $IL\text{-}17A^+$ cells in $CD4^+$ T cells from the in vitro culture system (*n*=6 replicates from two separate cell isolations). Data are means ± SD and are pooled from two independent experiments. ****P<0.0001 vs. Fc control group. NS, non-significant. One-way ANOVA with Dunnett's multiple comparisons test.

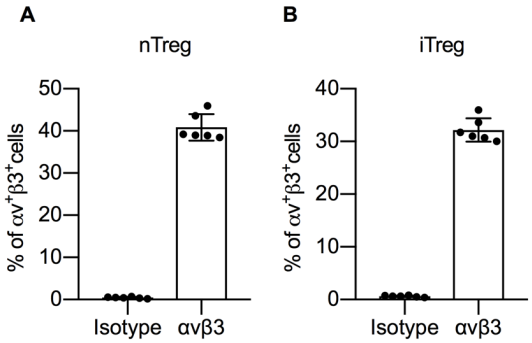

Supplemental Figure 10. αvβ3 expression on nTreg and iTreg cells. (A) Percentages of $\alpha v^+\beta 3^+$ cells in thymus derived natural Treg (nTreg) cells (*n*=6 mice per group) and **(B)** in in vitro-induced iTreg cells (*n*=6 replicates per group). Data are means ± SD and are pooled from two independent experiments.

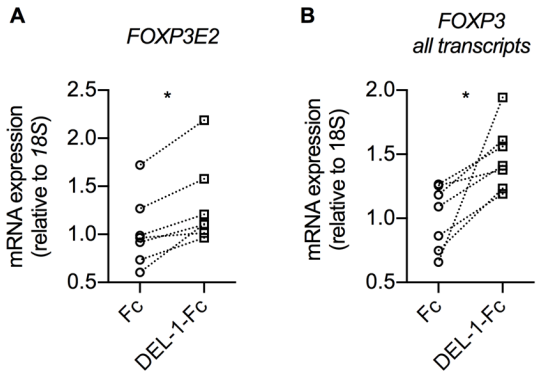

Supplemental Figure 11. DEL-1 increases the expression of *FOXP3E2* and all *FOXP3* transcripts in human iTreg cells. (A,B) Human Tconv cells were stimulated with anti-CD3/anti-CD28 (0.1 bead per cell) in vitro, in the presence of DEL-1-Fc or Fc control (each at 10 μg/ml). **(A)** Relative mRNA expression of *FOXP3* containing the exon 2 (*FOXP3E2*) and **(B)** *FOXP3* all transcripts (n=7 from seven independent experiments) was measured at 12 hrs of Tconv cell stimulation during iTreg cell generation, by real-time PCR. The pair of data for each individual is connected by a line. *P<0.05 vs. Fc control. Two-tailed paired Wilcoxon test.

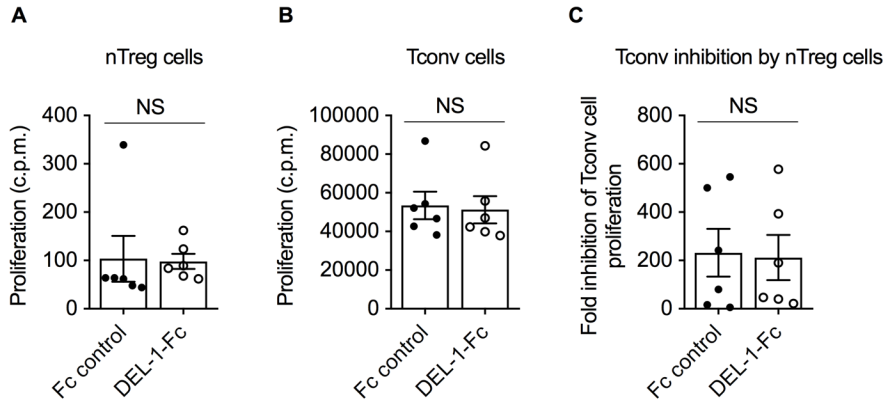

Supplemental Figure 12. DEL-1 does not affect the proliferation of nTreg and Tconv cells or the suppressive capacity of nTreg cells. Human nTreg (**A**) and Tconv (**B**) cells were stimulated with anti-CD3/anti-CD28 (0.2 bead per cell), in the presence of DEL-1-Fc or Fc control (each at 10 µg/ml) for 72 hrs. **(C)** Fold inhibition of Tconv cell proliferation co-cultured with nTreg cells for 72 hrs at a ratio of 1:1, in the presence of DEL-1-Fc or Fc control (each at 10 µg/ml), presented relative to results obtained for Tconv cells stimulated with anti-CD3/anti-CD28 (0.2 bead per cell) alone. **(A,B,C)** Data analysis of (**A**) nTreg and (**B**) Tconv cell proliferation and (**C**) fold inhibition of Tconv cell proliferation. Data are means ± SEM (*n*=6 from six independent experiments). NS, non-significant. Two-tailed paired Wilcoxon test.

Supplemental Table 1. Primers used for quantitative real-time PCR analysis.

Genes	Assay ID	Company
Mouse *Foxp3*	Mm00475162_m1	Thermo Fisher Scientific
Mouse *Runx1*	Mm01213404_m1	Thermo Fisher Scientific
Mouse *Runx3*	Mm00490666_m1	Thermo Fisher Scientific
Mouse *Cbfb*	Mm01251026_g1	Thermo Fisher Scientific
Mouse *Il6*	Mm00446190_m1	Thermo Fisher Scientific
Mouse *Il17a*	Mm00439618_m1	Thermo Fisher Scientific
Mouse *Tnfsf11*	Mm00441906_m1	Thermo Fisher Scientific
Mouse *Tgfb1*	Mm01178820_m1	Thermo Fisher Scientific
Mouse *Tgfb2*	Mm00436955_m1	Thermo Fisher Scientific
Mouse *Gapdh*	Mm99999915_g1	Thermo Fisher Scientific
Human *FOXP3* all transcripts	Hs00203958_m1	Thermo Fisher Scientific
Human *FOXP3E2*	Hs01092118_g1	Thermo Fisher Scientific
Human *RUNX1*	Hs02558380_s1	Thermo Fisher Scientific
Human *CBFB*	Hs00903431_g1	Thermo Fisher Scientific
Human *RNA18S5*	Hs03928990_g1	Thermo Fisher Scientific

Supplemental Table 2. Primers used for quantitative real-time PCR analysis of human and mouse iTreg methylation.

	Primers
Human/Mouse *Foxp3 CNS2* Fw	5’ – GACATCACCTACCACATCC – 3’
Human/Mouse *Foxp3 CNS2* Rev	5’ – TATCGGGGTCTGCATCTGG – 3’
Human *H19* Fw	5’ – GAGCCGCACCAGATCTTCAG – 3’
Human *H19* Rev	5’ – TTGGTGGAACACACTGTGATCA – 3’
Human *UBE2B* Fw	5’ – CTCAGGGGTGGATTGTTGAC – 3’
Human *UBE2B* Rev	5’ – TGTGGATTCAAAGACCACGA – 3’
Mouse *H19* Fw	5’ – CCCCAACTTTGCCATAAGTACGAT – 3’
Mouse *H19* Rev	5’ – GTCTGGTGATTTGCGCTTTCGTAT – 3’
Mouse *UBE2B* Fw	5’ – TGGAGCCCTTTTAAAAGCTC – 3’
Mouse *UBE2B* Rev	5’ – CCTGGGACTCACAATGTATAC – 3’